Sheet Thinning Prediction and Calculation in Incremental Sheet Forming

Harish K. Nirala and Anupam Agrawal

Abstract Incremental Sheet Forming (ISF) technique is an emerging process for die less forming. It has wide applications in many industries e.g., automobile and medical bone transplants. In ISF, forming of the sheet is done using Numerical Control (NC) single point forming tool, which incrementally deforms the sheet by highly localized plastic deformation. It gives better formability when compared with traditional forming processes, like deep drawing and spinning. ISF has few limitations out of which sheet thinning is one of the most critical limitations. In ISF, formability is generally measured by the limit of maximum formable wall angle and maximum permissible sheet thinning. Formability of the sheet during ISF or traditional forming processes can be presented by a Forming Limit Curve (FLC). The sheet thinning in ISF can be predicted through sine law. By assuming plastic incompressibility, sheet thinning can also be predicted by considering volume constancy concept. In this study, forming limit has been predicted for two wall profiles, viz., circular and elliptical wall. Further, a methodology has been presented as a way to predict and calculate sheet thinning during ISF. The developed methodology has been validated through numerical simulations followed by experimental investigations. An in-house Computer-Aided Manufacturing (CAM) module for incremental toolpath is developed for both simulations and experiments. The results are in correlation with considerable accuracy.

Keywords Incremental sheet forming (ISF) · FEA · Sheet thinning CAD/CAM · Sheet thinning models · FLC

H. K. Nirala · A. Agrawal (✉)
Department of Mechanical Engineering, Indian Institute of Technology Ropar, Rupnagar, Punjab 140001, India
e-mail: anupam@iitrpr.ac.in

H. K. Nirala
e-mail: harish.nirala@iitrpr.ac.in

S. S. Pande and U. S. Dixit (eds.), *Precision Product-Process Design and Optimization*, Lecture Notes on Multidisciplinary Industrial Engineering,
https://doi.org/10.1007/978-981-10-8767-7_15

Nomenclature

$\propto$, ø	Wall angle
x, y, and z	Coordinates
t_f	Final thickness
t_o	Initial thickness
f_t	Forming limit
v	Poisson's ratio

1 Introduction

Single Point Incremental Sheet Forming (SPISF) is a widely known alternative to traditional forming techniques. The sheet metal could be formed into desired symmetrical or asymmetrical shape without using any die. In this process, the sheet is clamped from its periphery on a suitable fixture mounted on a CNC machine and a hemispherical end shape forming tool is clamped to the machine spindle. The movement of forming tool over the sheet is controlled by the toolpath given as numerical code to the machine controller. The tool induces localized plastic deformation in the sheet (Young and Jeswiet 2004). These localized deformations are responsible for the forming of required geometry with higher formability as compared to conventional forming techniques. SPISF has drawn attention of manufacturing arena because it is very suitable and effective for small batches in production system (Jeswiet et al. 2005; Jackson and Allwood 2009). In 1967, a patent filed by Leszak initiated research in ISF (Leszak 1967). In 1978, work done by Mason at university of Nottingham gave a new direction to forming by ISF (Mason 1978). In 2001, Matsubara developed a double point ISF technique to improve its dimensional accuracy (Matsubara 2001). A comprehensive review of ISF is very effectively given by Jeswiet et al. (2005). Schematic representation of SPISF process is shown in Fig. 1.

Figure 1, briefly shows a SPISF process, a truncated cone geometry with a wall angle 'α' is being formed by an incremental spiral toolpath. The area of sheet metal which is in contact with the tool undergoes localized plastic deformation and results in sheet thinning. An intermediate geometry is also shown in the figure to give an idea of the deformation direction. A backing plate has been used in order to avoid undesired bending near the periphery of the geometry. Rotation of the tool is given in a clockwise direction with an angular velocity 'ω'.

This process has drawn the attention of many manufacturing research communities all around the world since last two decades. The reasons are greater process flexibility, improved formability and reduced forming forces when compared with conventional forming processes like deep-drawing, stretch forming and spinning. Ford Motor Company has recently released Ford Free Form Fabrication Technology (FFFFT) that uses Two-Point ISF (TPISF) for rapid prototyping of

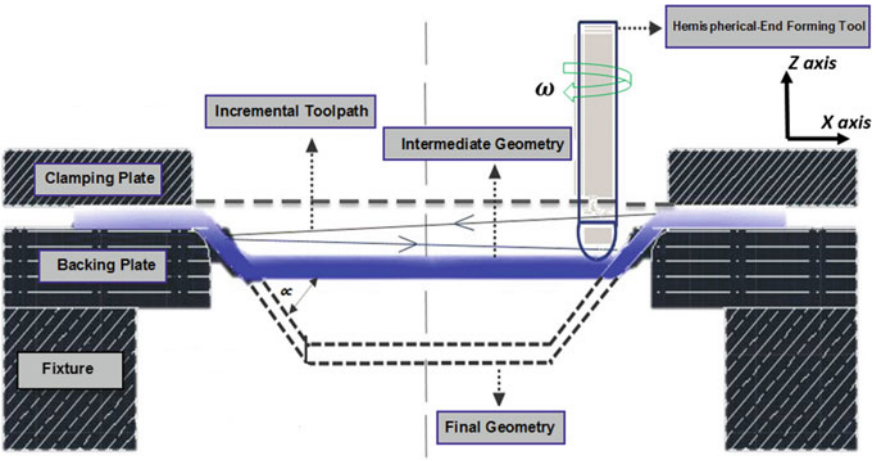

Fig. 1 Schematic representation of SPISF process

automobile parts.[1] When in SPISF any full or partial die is used then the process is termed as Two-Point Incremental Sheet Forming (TPISF). In SPISF there is only one contact point between the sheet and the tool while in TPISF there are two contact points. In TPISF, first contact point is in between forming tool and the inner surface of geometry and other contact point is between outer surface of geometry and die used during forming. ISF has potential application in the medical bone prosthesis. Bone implants with some cavity can be formed by using ISF process. Literature (Lu et al. 2015) shows its application in cranioplasty (Bagudanch et al. 2015), knee arthroplasty (Bhoyar and Borade 2015; Eksteen 2013; Eksteen and Van der Merwe 2012), denture plate (Milutinovića et al. 2014), maxillofacial implant (Araújo et al. 2013), heel bone replacement (Ambrogio et al. 2005) and many more. These implants need a customized fabrication, which can be possible through a flexible process like ISF. Figure 2, shows some application of ISF in different manufacturing sectors. The deformation mechanism of ISF includes, biaxial stretching at the start point, at the corners and at each increment in the negative z direction. The deformation, when the tool travels horizontally or spirally along the formed profile, is plain-strain stretching and shearing (Jackson and Allwood 2009). The deformation mechanism in ISF also includes pure bending of the sheet while forming (Jackson and Allwood 2009). Further, the deformation mechanism in conventional drawing process is purely biaxial, due to which the stress triaxial condition necessary for fracture is achieved far earlier in conventional forming than in incremental forming. Process parameters like feed rate, spindle speed, tool diameter, incremental depth, forming angle, sheet thickness and toolpath will have a

[1] http://corporate.ford.com/news-center/press-releases-detail/pr-ford-develops-advanced-technology-38244, 10 August, 2014, 8:30 pm IST.

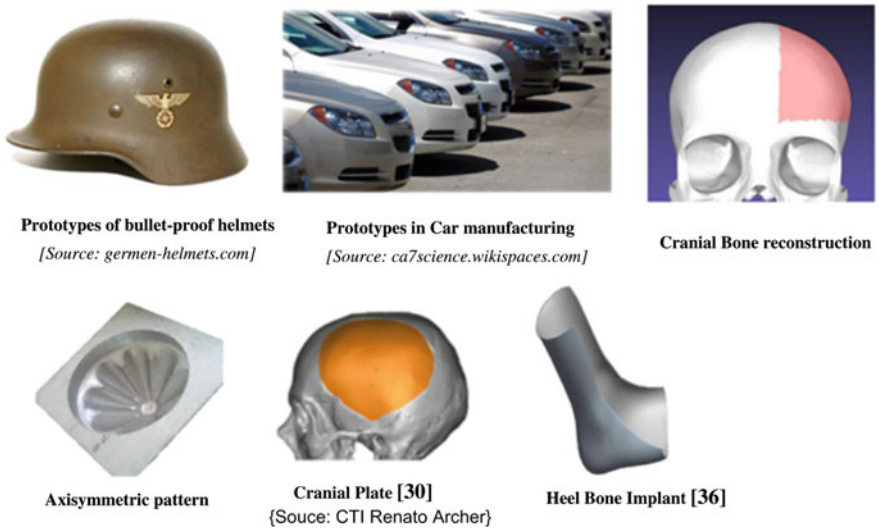

Fig. 2 Some applications of ISF Bagudanch et al. (2015), Ambrogio et al. (2005)

significant effect on the formability achieved (Kim and Park 2002; Gatea et al. 2016). In SPISF, formability of the sheet is generally presented by a Forming Limit Diagram (FLD). FLCs are generally plotted in a principal space of major and minor strain $(\varepsilon_1, \varepsilon_2)$. In Fig. 3, formability comparison between deep drawing and incremental sheet forming is presented (Silva et al. 2008a). Figure 3, clearly shows that ISF gives better formability than traditional forming techniques in a principal strain space (Silva et al. 2008b). There are few limitations of this process also like geometrical inaccuracy, sheet thinning, undesired bending and spring back. Out of these limitations, sheet thinning is the most critical limitation. Hence, it becomes very necessary to study sheet tinning in ISF. From literature, it has been found that sine law can be used to predict the sheet thickness variation along the formed profile (Duflou et al. 2008). The sine law can be utilized to predict the final part thickness T_{final} from the unprocessed sheet thickness T_{Initial} and the part wall angle $\propto$ (Duflou et al. 2008). From Eq. (1), one can conclude that, as the wall angle (α) of the formed profile increases, the final profile thickness T_{final} decreases.

$$T_{\text{final}} = T_{\text{Initial}} \sin(90^\circ - \propto) \tag{1}$$

According to sine law, it is not possible to form vertical wall $(\alpha = 90^\circ)$, as it gives final sheet thickness as zero. However, researchers have successfully formed vertical walls using multistage ISF. When the sheet is being deformed strain hardening effect appears which reduces the deformation capability of the sheet. There will be more strain hardening, when deformation imposed on the sheet is large as in single-stage SPISF process. When few intermediate stages are introduced then the strain hardening effect will reduce and formability will improve

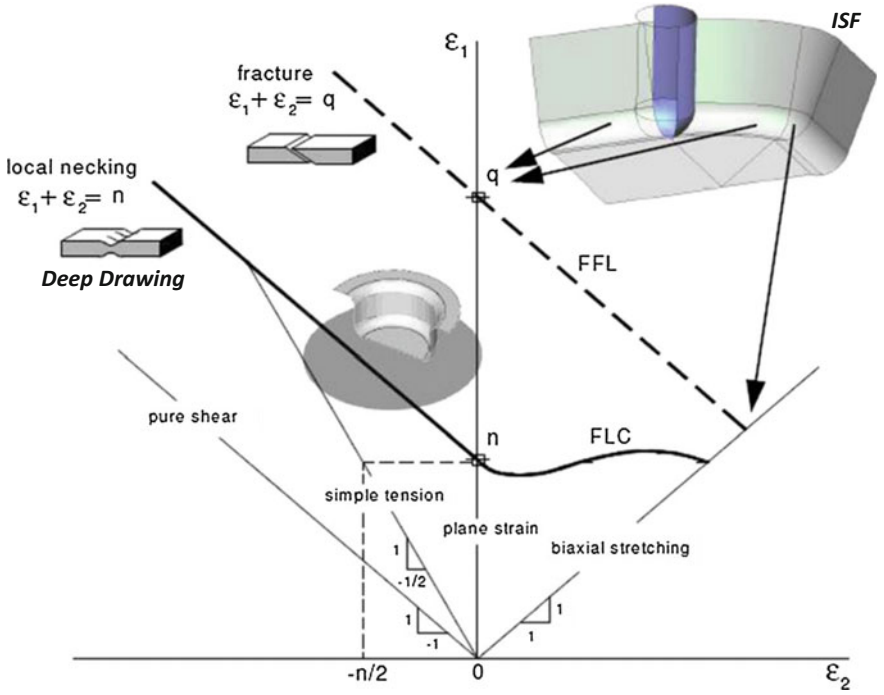

Fig. 3 Forming limit diagram for conventional forming and ISF (Silva et al. 2008a)

because the overall deformation will now be distributed among these intermediate stages (Nirala et al. 2017). Young and Jesweit (2004), investigated a double pass SPISF process. In double pass SPISF process, a preform geometry is formed before forming the final desired geometry. The formability of geometry formed by using double pass ISF process was higher than the single pass ISF process. The final thickness in double pass ISF can be given by:

$$T_f = T_p \frac{\sin(\propto)}{\sin(\phi)} \tag{2}$$

In Eq. (2), T_P is the thickness of preform obtained from sine law, ø is the wall angle of preform geometry, $\propto$ is the wall angle of final geometry, and T_f is the thickness of final geometry. Liu et al. (2013, 2014), developed some strategies for multistage ISF and conducted plane strain deformation analysis to analyze the strain distribution in these strategies. Filice (2006), developed some analytical relations to predict sheet thickness by the concept of volume constancy. Step features observed while forming with multistage SPISF strategy (Liu et al. 2014; Xu et al. 2012). Bambach (2010), given a more generalized sine law, which considers the evolution of surface from the sheet blank (Bambach 2010). Mirnia et al. (2014) have done modeling of SPISF using sequential limit analysis to predict the sheet thickness

(Mirnia et al. 2014). Cao et al. (2015) have developed an efficient method to predict sheet thickness in multistage incremental sheet forming. Lu et al. (2015) reinvestigate the deformation mechanism in ISF by the concept of stress triaxiality. Ambrogio et al. (2017) proposed a robust meta-modeling technique for the crucial problem of localized thinning. Skjodt et al. (2010), studied the formability of 1 mm AA1050-O sheets, their study includes evaluation of strain paths and fracture strains in single and multistage SPISF process. Silva et al. (2011), revisited the failure mechanism in ISF, they considered the influence of process parameters like tool diameter on fracture initiation and propagation. Silva et al. (2011), very effectively presented the state of stress and strain in plane strain and biaxial strain conditions, also the influence of tool diameter on localized deformation is presented. The strain evolution is then verified for truncated cone and truncated pyramid by experiments and shown using Forming Limit Curves (FLC's). Over the time, several techniques have been developed to improve the formability of ISF process like, laser assisted ISF (Jeswiet et al. 2005) and electrically assisted ISF (Nguyen-Tran et al. 2015). There are many online thickness measurement techniques available in the literature, like thickness measurement by using Digital Image Correlation (DIC) (Hild and Roux 2006; Chu et al. 1985), Dejardin et al. (2010), emphasized that for the industrialization and optimization of ISF, online monitoring of sheet thinning is very necessary. Paniti and Paroczi (2011), developed a noncontact type thickness measurement device based on Hall-effect. The methodology developed by these researchers is effective, but some are complex and time taking, when it comes to implementation. The present methodology can predict and calculate sheet thickness of formed profile in an effective, simpler and easy manner.

This research work presents a methodology to predict and calculate sheet thinning in single-stage ISF process. The sheet is assumed to be isotropic and incompressible, the deformation is only considered as plane strain, and the effect of process parameters like feed, tool diameter, etc., is neglected. To predict the sheet thinning in single stage ISF, a further improvement in the model proposed by Hussain and Gao (2007) is proposed for better flexibility and implementation. These analytical models are discussed in detail in further sections of this study. Anon-contact-based technique is presented to calculate sheet thinning in single stage ISF. This technique uses the strain distribution data after experiments and fits that data into a theoretical relation (Sect. 3). The effectiveness of the abovementioned models is then verified through simulations followed by real experiments.

2 Thickness Prediction

In this section, analytical model to predict sheet thinning along forming depth in ISF is discussed. In this model, the effect of elastic behavior of the sheet is neglected and the sheet is considered as isotropic. The deformation is considered as plane strain deformation. The thickness prediction results are then compared with

experimental and FEA results, in results and discussion section, which describes the effectiveness of the proposed model. Circular and elliptical wall profiles are formed using ISF. In circular wall profile, wall angle varies from 30° to 75° and for elliptical wall profile, wall angle varies from 20° to 85°. For simplicity, the elastic behavior of the sheet is neglected, even it effects the sheet when unclamped from the fixture. The overspinning of the sheet during forming is neglected, overspinning refers to sheet thinning by compressive stresses applied by the forming tool. The material behavior and friction between the sheet and tool are neglected. On the whole, the problem is plane strain type. There are certain limitations of the model proposed by Hussain and Gao (2007), it specifically calculates the thinning limit of the formed geometry. It requires coordinate data points of the toolpath at every incremental depth, hence, use of commercial CAM software is not advisable to implement the concept. The quality of the formed part is very much dependent on the toolpath strategy. At present, many existing CAM (Computer Aided Manufacturing) software packages can be used to generate the toolpath for SPISF process like CATIA, Siemens NX 8.0 and Delcam PowerMILL 10. To overcome the abovementioned limitations an in-house CAM module is developed which is capable of giving constant z toolpaths for any axisymmetric component. The CAM module is subdivided into two sections. The first program calculates the wall angle at every increment for a generalized equation driven curve by calculating the slope at every incremental depth (Eq. 7). The second program, generates a 3D incremental toolpath, for any choice of incremental depth, for the required geometry. In order to calculate the wall angle of any profile, one needs to know the equation of that curve first. Most of the equation driven curves like parabola, hyperbola, and spline have their predefined equations. For free-form curves (asymmetric), rational Bezier curves can be used for describing the 2D cross-section of the profiles to be formed by ISF. A rational Bezier curve of nth degree can be defined as (Cao et al. 2015; Piegl and Tiller 1997):

$$c(u) = \frac{\sum_{i=0}^{n} B_{i,n}(u)\omega_i P_i}{\sum_{i=0}^{n} B_{i,n}(u)\omega_i} 0 \le u \le 1 \tag{3}$$

where, $P_i = (x_i, y_i, z_i)$ are the control points, and ω_i is the scalar for each point. In Eq. (3), the basis function $B_{i,n}(u)$ is the Bernstein polynomial with nth degree. However, in this research work, curvilinear geometric profiles with predefined equations (circular and elliptical) for their curves have been used. A pseudo code for incremental toolpath generation for any profile in *MATLAB*® is given in the Appendix. Also, procedure to conduct numerical simulations and experiments from this CAM module is shown in Fig. 4.

In Fig. 5, a circular generatrix profile is shown, A and C are the extreme ends of the profile, while B is the point where crack has been occurred, h is the forming depth of the profile. Thickness (t_f) and amount of thinning (f_t) at failure point 'B' are given by following equations:

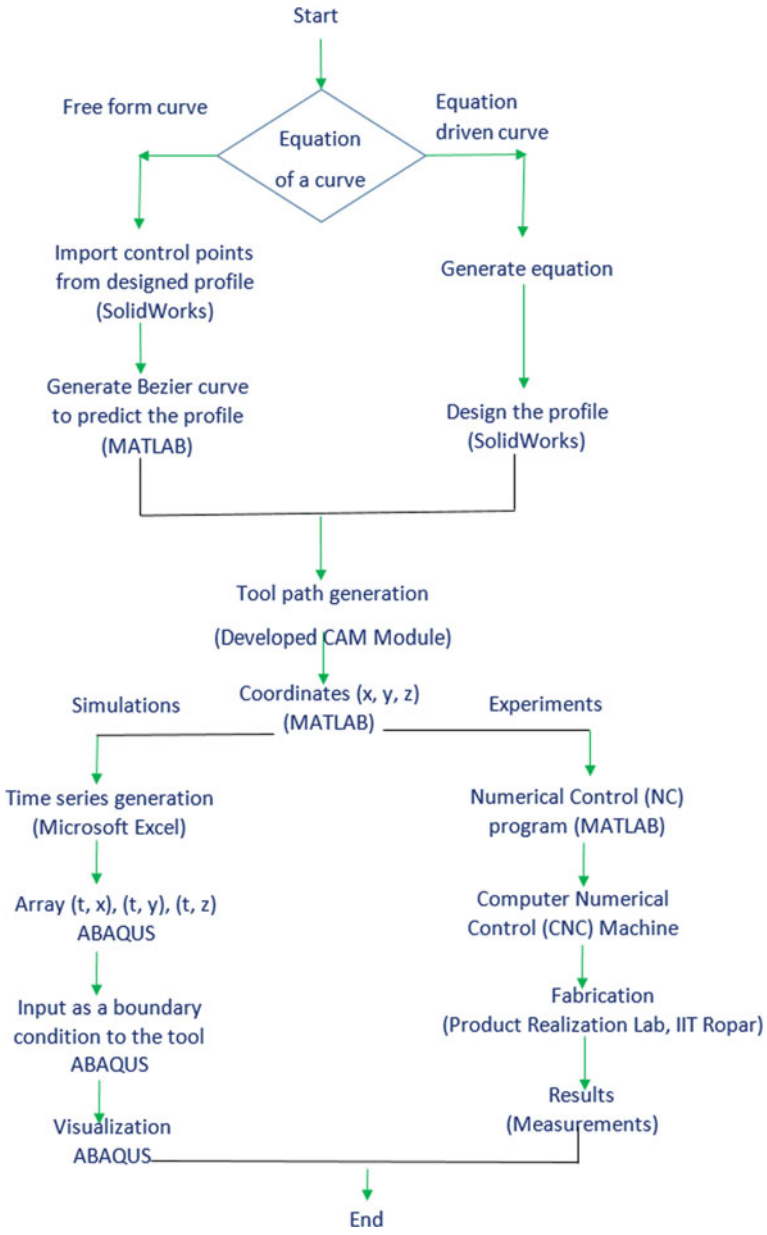

Fig. 4 Flowchart for toolpath generation, simulations and experiments

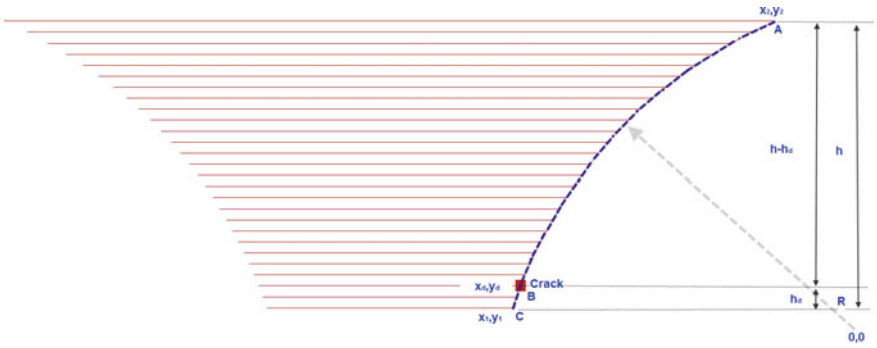

Fig. 5 Illustration of a generatrix with MATLAB toolpath

$$t_f = \frac{t_0}{R}(y_2 - \{h - h_d\}) \tag{4}$$

$$f_t = 100\left[1 - \frac{1}{R}(y_2 - \{h - h_d\})\right] \tag{5}$$

where, t_f is the final thickness, t_0 is the initial thickness and f_t is the amount of thinning. One can predict the thickness for overall profile, based on the modifications (Eqs. 6 and 7) in conjunction with abovementioned equations (Eqs. 4 and 5). Based on the below modifications (Eqs. 6 and 7) in conjunction with abovementioned equations. Equations (6) and (7), give a modified version to the sine law, which is capable of predicting sheet thickness of asymmetric curvilinear wall profiles.

$$\frac{\{y_2 - \{h - h_d\}\}}{R} = \sin(90 - \propto) \tag{6}$$

where,

$$\propto = \tan^{-1}\frac{(\mathrm{d}y/\mathrm{d}z)}{(\mathrm{d}z/\mathrm{d}x)} \tag{7}$$

The major benefits of this model over other models are as follows:

- It is capable of predicting thickness of any geometric profile.
- It is basically an improved version of sine law for curvilinear profiles.
- It is capable of predicting thickness at any forming depth.
- Continuous thickness prediction throughout the profile.
- Predict thickness even when there is variation in step depth of incremental toolpath.

3 Thickness Calculation

The most common and effective methods of measuring strain or plastic deformation are grid marking, extensometers, strain gauges and ultrasound thickness measurements. Grid deformation analysis is a most common and easy method of measuring the deformation of a formed sheet (Kim and Lee 1996). Grid marking consists of marking square or circular grid pattern over the sheet metal blank (Diameter of circle ranges between 1 and 8 mm, which depends on the size of the component) (Hariharan and Balaji 2009).[2] The incremental sheet forming process usually considered as plane strain deformation process because the thickness of the sheet is generally very less as compared to other dimensions of the sheet. Due to the plane strain nature of deformation, surface strains measurement becomes very important. Forming limit diagram can also be plotted using the calculated surface strains. In this study, a simplified technique (Eqs. 8–11) is presented to measure thinning of the sheet by using strains in meridional direction (ε_{11}), circumferential direction (ε_{22}) and through thickness direction (ε_{33}). In Eq. (8), E is the modulus of elasticity and v is the Poisson's ratio. In Eq. (11), t_0 is the initial sheet thickness and t_f is the final sheet thickness. This method of thickness prediction is basically employed by ABAQUS,[3] it computes the lateral and longitudinal strain for every shell element undergoing plane strain deformation. In this study, the present method has been used in conjunction with the strain distribution data collected from the grid deformation analysis.

$$\frac{Ev}{(1-2v)(1+v)}\varepsilon_{11} + \frac{Ev}{(1-2v)(1+v)}\varepsilon_{22} + \frac{Ev}{(1-2v)(1+v)}\varepsilon_{33} = 0 \tag{8}$$

$$\varepsilon_{33} = -\left(\frac{v}{1-v}\right)(\varepsilon_{11} + \varepsilon_{22}) \tag{9}$$

$$\ln\frac{t_f}{t_0} = \varepsilon_{33} \tag{10}$$

$$t_f = t_0 e^{\varepsilon_{33}} \tag{11}$$

The final sheet thickness (t_f) of curvilinear profiles, calculated from the calculation model is then compared with FEA and experimental results. A comparison of the effectiveness of this method is discussed further in this study.

[2] http://lectroetch.com/product-category/grid-marking-equipment/, 31st July, 2017, 1:45 am. IST.

[3] ABAQUS/Explicit Theory Manual Version 6.3, vol. 1–2, 2002.

4 Finite Element Analysis

Finite Element Analysis (FEA) is a tool to approximately predict the results of a process. The accuracy of results in ABAQUS depends on the quality of technical data available as an input to the FEA model. Few parameters like E, v material density, strain hardening exponent, friction coefficient and the material constant need to be accurately known for any sheet metal forming simulation. Meshing effects the accuracy of results and computational time. Generally, adaptive meshing is preferred to optimize computational time with the accuracy of results. A 3D elastic-plastic FEM (Finite Element Model) for ISF is established in ABAQUS software suite. An isotropic sheet blank with 'S4R' shell elements is considered for this study. The forming tool is considered as a rigid body. The elastic and plastic properties of the sheet blank (Aluminium 6106-T6) are considered during simulations. The thicknesses of the sheet and tool diameter are taken as 1 and 8 mm respectively for the simulations and experiments. The interaction between the sheet and forming tool is implemented by a pure master-slave contact algorithm. Additionally, the coefficient of friction between blank and the tool is taken as 0.1 by using Coulomb's law of friction (Li et al. 2012). The forming tool moves in a 3D path according to the boundary conditions assigned to it in x, y, and z coordinates. The time series generation for the amplitude of these boundary conditions is based on Eqs. (12) and (13); where x, y, and z are the coordinates of the toolpath are extracted from MATLAB (Nirala et al. 2015).

$$\text{Time step } (t) = \frac{D(\text{Step distance})}{\text{Velocity of tool } (v)} \tag{12}$$

$$\text{Step distance } (D) = \sqrt{(x_2 - x_1)^2 + (y_2 - y_1)^2 + (z_2 - z_1)^2} \tag{13}$$

The time step and step distance used during simulations are derived from Eqs. (12) and (13). An array of time steps and x, y, z coordinates are established while assigning boundary condition to the forming tool. As a result, the toolpath in the real process is same as that in simulations. The velocity of forming tool in simulations is generally taken more than the real process but below a critical value in order to reduce computational time in simulations (Hirt et al. 2005; Hadoush and Van den Boogaard 2008). A simple setup for carrying out simulations is shown in Fig. 6. The toolpath designed in MATLAB and FEA results of thickness distribution for circular and elliptical wall profiles are shown in Fig. 7. In Fig. 7, the output variable (sheet thickness) values for shell elements are averaged within 75% in correlation with each other (nodal averaging scheme in Abaqus).

The circular and elliptical wall profiles are simulated up to a designed forming depth of 30 mm. From the results of the simulations, it is quite clear that the

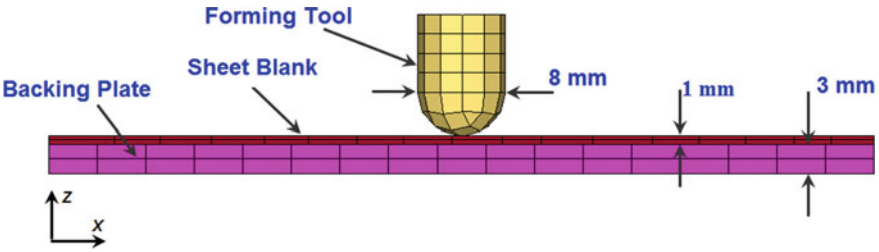

Fig. 6 Numerical simulation setup for ISF

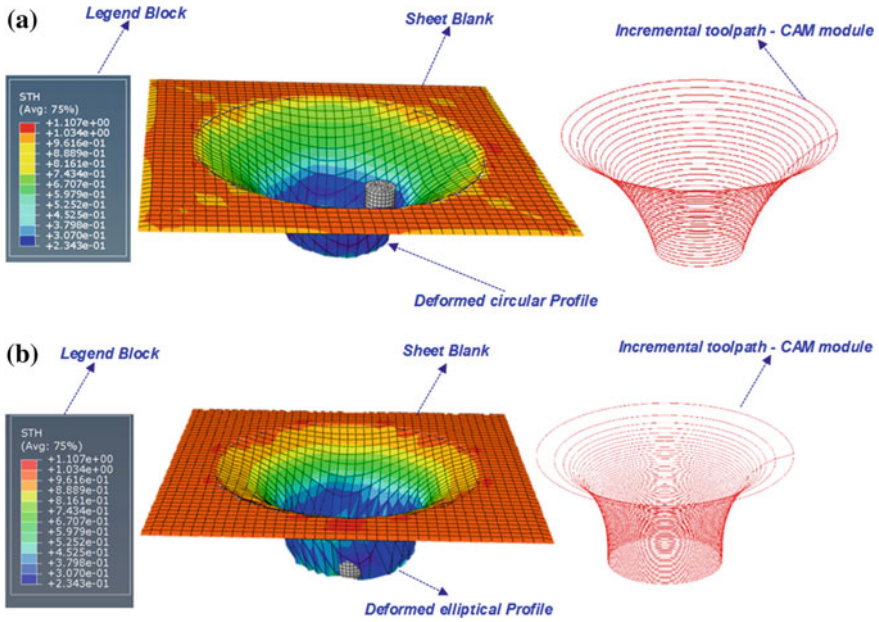

Fig. 7 FEA results of shell thickness for **a** circular wall, **b** elliptical wall profiles

deformation in SPISF is plane deformation i.e., stretching in the radial direction and compressing in the normal direction. The results of the simulations are well in accordance with the previous studies (Nirala et al. 2015; Han and Mo 2008). In previous studies, the authors have conducted similar simulations and found similar decreasing trends of sheet thickness along forming depth. In all three cases, the minimum thickness is observed near the base of the formed profile. From the stress-strain relationship, it can be concluded and also observed in simulations that over the formed profiles, where the strain is higher, stress will also be reported as

higher (Fig. 7). Hence, in simulated profiles, maximum stress will be observed in the region of maximum thinning (Fig. 7). The advantage of using numerical analysis is to predict the sheet thinning (Nirala et al. 2017) in ISF before doing real experiments. Fine meshing in simulations gives accurate results (percentage error <5%) but fine meshing takes very long computational time. It takes few days or even weeks to do the analysis of a geometry when very fine meshing is used (shell element size <0.2 mm, for considered geometries).

5 Experimental Exploration

One cannot solely depend on simulation results because every solver of a numerical analysis software gives different results for the same problem. This is primarily due to the various assumptions considered while designing a numerical analysis setup. Hence, the results from the simulations need to be verified by the experiments for confirmation. The x, y and z coordinate extracted from the toolpath program can be utilized to make an NC part program for a 3 axis vertical milling machine (here, BFW, Model: VF 30 CNC VS). A fixture to conduct the experiments is designed and fabricated as shown in Fig. 8. A backing plate is generally used to avoid undesired bending near the periphery of the geometry (Duflou et al. 2008). For each of the experiments, a tungsten carbide made hemispherical end shape forming tool with 8 mm diameter is chosen. The sheet blanks used in the present study are 1-mm-thick aluminum sheets (70 × 70, Al 6101-T6). Al 6101-T6 is a commonly used alloy in aerospace, aviation, and marine industry. The mechanical properties of Al 6101-T6 are shown in Table 1. Feed of 500 mm/min is provided to the tool which is rotating at 500 RPM.

The sheet metal blanks of aluminum alloy are prepared by trimming operation and then clamped over the fabricated fixture. Serigraphy method is used to print the

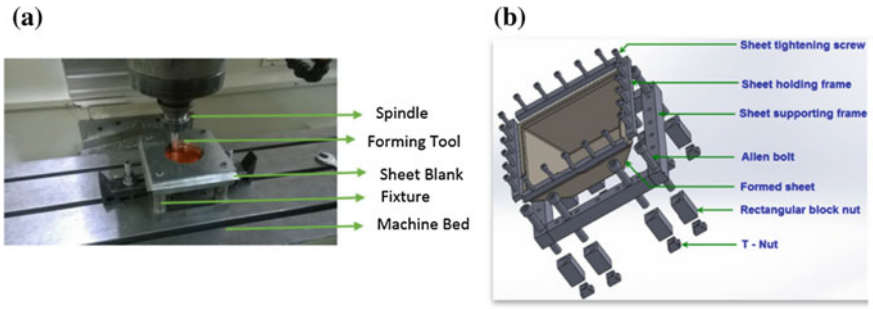

Fig. 8 Fixture for ISF. **a** Experimental setup and **b** CAD model

Table 1 Mechanical properties of Aluminium 6101-T6

Properties	Magnitude
Density	2.7 g/cc
Melting point	600 °C
Poisson's ratio	0.33
Tensile strength	97 MPa
Modulus of elasticity	70 GPa
Yield strength	76 GPa

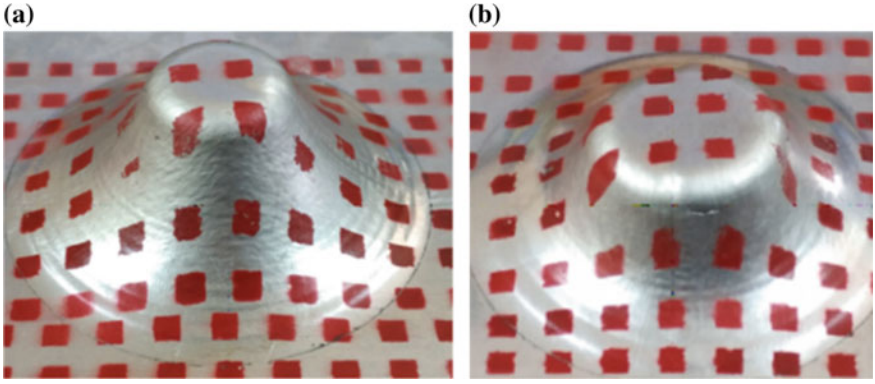

Fig. 9 Formed profiles. **a** Circular wall and **b** elliptical wall

grid pattern over the sheet. This method is one of the easiest and cost-effective methods of grid marking (Hariharan and Balaji 2009). This is done in order to measure the surface strains after deformation. The profiles are chosen so that crack can be observed, which the most critical limitation of this process. Multiple experiments were carried out for the different range of profiles, so that the crack initiation could be observed at shallow forming depth. Formed components, circular and elliptical wall profiles, by SPISF are shown in Fig. 9. To obtain the thickness profiles, the formed geometries are mounted from the fixture and their cut sections are prepared by using Electrical Discharge Machining (EDM). The thickness profiles are prepared by measuring the sheet thickness of formed geometries along forming depth using a micrometer with least count ± 1 μm.

6 Results and Discussion

In this section, results of thickness and strain distribution with forming depth are presented and discussed. Also, a comparison based study of the formed components (circular and elliptical wall profiles) is presented using Fracture Forming Limit

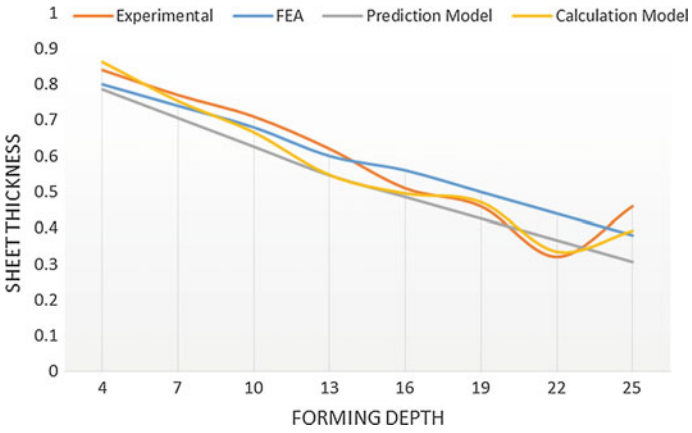

Fig. 10 Thickness distribution comparison for circular wall profile (Nirala and Agrawal 2016)

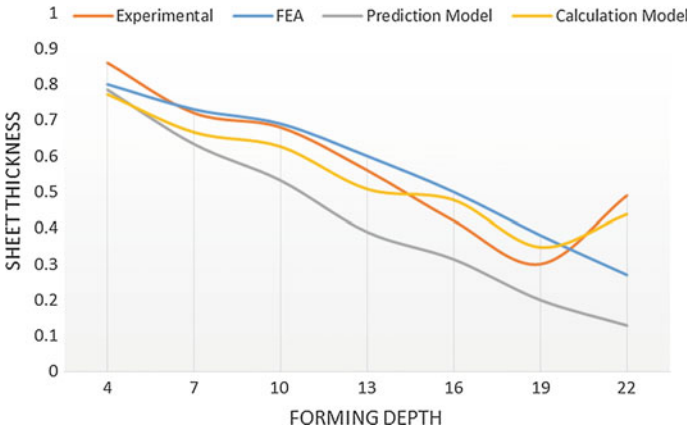

Fig. 11 Thickness distribution comparison for elliptical wall profile (Nirala and Agrawal 2016)

(FFL) diagram. From Figs. 10 and 11, it can be observed that the thickness of wall reduces with forming depth. The main reasons for thickness reduction are stretching, shearing and squeezing of the sheet in meridional, circumferential and through-thickness directions respectively (Jackson and Allwood 2009). It has been observed during experiments that the thickness near the base is slightly more than the region where the crack has occurred. The possible reason for this can be the accumulation of stretched material near the tool contact point. FEA and prediction model do not consider this factor which results in higher average percentage errors.

However, up to crack region, the values of percentage error remain below 10%. From Fig. 10, circular wall profile, the average percentage errors of FEA, prediction model and calculation model from experimental data are 11, 12, and 5% respectively. From Fig. 11, elliptical wall profile, the average percentage errors of FEA, Prediction model and calculation model on comparison with experimental data are 15, 29, and 10% respectively.

It took nearly 48 h to complete one FEA simulation of the single stage ISF. One can clearly see (Figs. 10 and 11) that the prediction model can be used over FEA to predict the approximate thickness distribution up to crack initiation. Calculation model can be used over experimental method to calculate thickness distribution. On comparing Figs. 10 and 11, it can be seen that the maximum forming depth achieved before crack initiation for the circular and elliptical wall is 25 and 22 mm respectively. Repeatability tests were also conducted to come to any conclusion. Hence, it can be concluded from the available results that, the prediction and calculation models fit better for the curvilinear profiles, where the wall angle variation from top to bottom of the wall is less (circular wall profile). For curvilinear profiles, with the high variation of wall angle from top to bottom of the wall (elliptical profile), the proposed models show high variance from actual experimental results.

Figure 12, shows the Fracture Forming Limit (FFL) diagram containing the Forming Limit Curve (FLC). The FLC is plotted from the data available in the

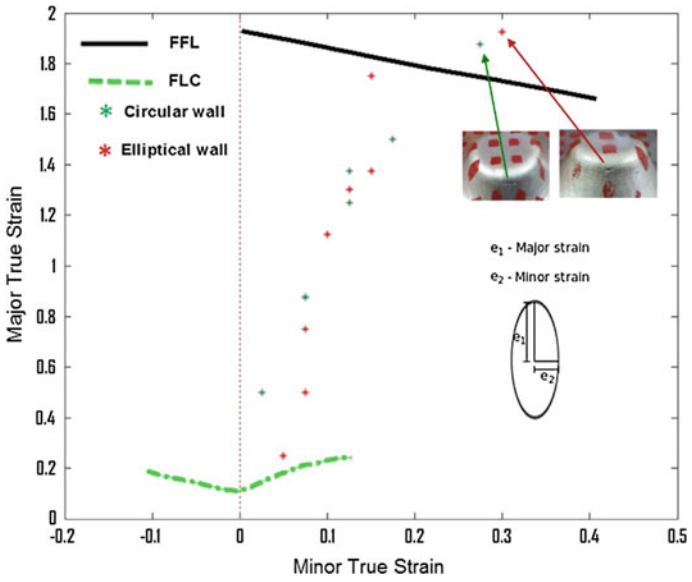

Fig. 12 FFL comparison for circular wall and elliptical wall (Nirala and Agrawal 2016)

literature, which was collected by conducting a combination of simple tensile test and Dome test (Silva et al. 2011). The reason of showing FLC in this study is to highlight the higher formability in ISF. Sheet cracked in the case of circular and elliptical wall profiles, whereas conical geometry successfully formed without any fracture. The points where the crack is observed are shown above the FFL line. In this study, analytical model available in the literature (Duflou et al. 2008; Hussain and Gao 2007), for thickness prediction is modified. Also, the thickness calculation model available in the literature (Filice 2006) is further derived and implemented using grid deformation analysis. However, the developed methodology by which this study has been conducted has not been found in the available literature.

7 Summary

In this work, a methodology is presented to predict and calculate the sheet thickness for the components fabricated by ISF process. The prediction model is developed to predict the sheet thickness before real experiments, while calculation model is developed to calculate the sheet thickness after real experiments.

- Thickness prediction model can predict sheet thickness under acceptable limits (approximate average % error—15%) up to crack initiation depth.
- Thickness calculation model can calculate the thickness within acceptable limits up to full forming depth.
- For a curvilinear profile, when the range of angle between two extreme ends is less and not very steep then the analytical models give better results. The range of angle between two extreme ends of the circular profile is less than the elliptical profile. Hence, results in the circular profile are better than the elliptical profile.
- The results from analytical models and calculation models are in good agreement with FEA and experimental results.
- For future study, material modeling using advanced material models like GTN, to predict damage initiation and propagation in single stage can be implemented in conjunction with developed prediction and calculation models.

Appendix

Pseudo Code

```
clc; clear all; clear;
Decide a constant value of stretching / Scallop Height; %For variable increment in negative z direction
Create empty arrays for x, y and z values;
Create an array for calculating wall angle at every increment;
Define initial constant step depth;
Define major base radius=r;
Program of wall angle (theta) calculation        % Based on equation 7
Forming Depth = 0;
While (angle >initial wall angle && angle<final wall angle)
    Call program of wall angle calculation;
        Generation of profile contour with forming depth
    Forming depth = Forming depth + step depth;
    If (depth>required depth)
        Break;
    End
                                                 End
```

References

Ambrogio, G., L. De Napoli, L. Filice, F. Gagliardi, and M. Muzzupappa. 2005. Application of incremental forming process for high customised medical product manufacturing. *Journal of Materials Processing Technology* 162: 156–162.

Ambrogio, G., C. Ciancio, L. Filice, and F. Gagliardi. 2017. Innovative metamodelling-based process design for manufacturing: an application to Incremental Sheet Forming. *International Journal of Material Forming* 10 (3): 279–286.

Araújo, R., P. Teixeira, M.B. Silva, A. Reis, and P. Martins. 2013. Single point incremental forming of a medical implant. *Key Engineering Materials* 554: 1388–1393. Trans Tech Publications.

Bagudanch, I., L.M. Lozano-Sánchez, L. Puigpinós, M. Sabater, L.E. Elizalde, A. Elías-Zúñiga, and M.L. Garcia-Romeu. 2015. Manufacturing of polymeric biocompatible cranial geometry by single point incremental forming. *Procedia Engineering* 132: 267–273.

Bambach, M. 2010. A geometrical model of the kinematics of incremental sheet forming for the prediction of membrane strains and sheet thickness. *Journal of Materials Processing Technology* 210 (12): 1562–1573.

Bhoyar, P.K., and A.B. Borade. 2015. The use of single point incremental forming for customized implants of unicondylar knee arthroplasty: a review. *Research on Biomedical Engineering* 31 (4): 352–357.

Cao, T., B. Lu, D. Xu, H. Zhang, J. Chen, H. Long, and J. Cao. 2015. An efficient method for thickness prediction in multi-pass incremental sheet forming. *The International Journal of Advanced Manufacturing Technology* 77 (1–4): 469–483.

Chu, T.C., W.F. Ranson, and M.A. Sutton. 1985. Applications of digital-image-correlation techniques to experimental mechanics. *Experimental Mechanics* 25 (3): 232–244.

Dejardin, S., Gelin, J.-C., Thibaud, S: On-line thickness measurement in incremental sheet forming process. In *Proceedings of the 13th International Conference on Metal Forming, Toyohashi*, 19–22 Sept 2010, 938–941.

Duflou, J.R., J. Verbert, B. Belkassem, J. Gu, H. Sol, C. Henrard, and A.M. Habraken. 2008. Process window enhancement for single point incremental forming through multi-step toolpaths. *CIRP Annals-Manufacturing Technology* 57 (1): 253–256.

Eksteen, P. D. W. 2013. *Development of incrementally formed patient-specific titanium knee prosthesis*. Doctoral dissertation, Stellenbosch: Stellenbosch University).

Eksteen, P.D.W., and A. Van der Merwe. 2012. Incremental sheet forming (ISF) in the manufacturing of titanium based plate implants in the bio-medical sector. *Computers and Industrial Engineering* 42: 15–18.

Filice, L. 2006. A phenomenology-based approach for modelling material thinning and formability in incremental forming of cylindrical parts. *Proceedings of the Institution of Mechanical Engineers, Part B: Journal of Engineering Manufacture* 220 (9): 1449–1455.

Gatea, S., H. Ou, and G. McCartney. 2016. Review on the influence of process parameters in incremental sheet forming. *International Journal of Advanced Manufacturing Technology* 87 (1): 479–499.

Hadoush, A., and A.H. Van den Boogaard. 2008. Time reduction in implicit single point incremental sheet forming simulation by refinement-derefinement. *International Journal of Material Forming* 1: 1167–1170.

Han, F., and J.H. Mo. 2008. Numerical simulation and experimental investigation of incremental sheet forming process. *Journal of Central South University of Technology* 15 (5): 581–587.

Hariharan, K., and C. Balaji. 2009. Material optimization: A case study using sheet metal-forming analysis. *Journal of Materials Processing Technology* 209 (1): 324–331.

Hild, F., and S. Roux. 2006. Digital image correlation: from displacement measurement to identification of elastic properties—A review. *Strain* 42 (2): 69–80.

Hirt, G., J. Ames, and M. Bambach. 2005. A new forming strategy to realize parts designed for deep-drawing by incremental CNC sheet forming. *Steel Research International* 76 (2–3): 160–166.

Hussain, G., and L. Gao. 2007. A novel method to test the thinning limits of sheet metals in negative incremental forming. *International Journal of Machine Tools and Manufacture* 47 (3): 419–435.

Jackson, K., and J. Allwood. 2009. The mechanics of incremental sheet forming. *Journal of Materials Processing Technology* 209 (3): 1158–1174.

Jeswiet, J., F. Micari, G. Hirt, A. Bramley, J. Duflou, and J. Allwood. 2005. Asymmetric single point incremental forming of sheet metal. *CIRP Annals-Manufacturing Technology* 54 (2): 88–114.

Kim H. J., and Lee D. 1996. Further development of experimental methods to verify computer simulations. In *Proceedings of NUMISHEET, Dearbom, Michigan, USA*, 316–323.

Kim, Y.H., and J.J. Park. 2002. Effect of process parameters on formability in incremental forming of sheet metal. *Journal of Materials Processing Technology* 130: 42–46.

Leszak, E. 1967. U.S. Patent No. 3,342,051. Washington, DC: U.S. Patent and Trademark Office.

Li, J.C., L.I. Chong, and T.G. Zhou. 2012. Thickness distribution and mechanical property of sheet metal incremental forming based on numerical simulation. *Transactions of Nonferrous Metals Society of China* 22: s54–s60.

Liu, Z., Y. Li, and P.A. Meehan. 2013. Vertical wall formation and material flow control for incremental sheet forming by revisiting multi-stage deformation path strategies. *Materials and Manufacturing Processes* 28 (5): 562–571.

Liu, Z., W.J. Daniel, Y. Li, S. Liu, and P.A. Meehan. 2014. Multi-pass deformation design for incremental sheet forming: Analytical modeling, finite element analysis and experimental validation. *Journal of Materials Processing Technology* 214 (3): 620–634.

Lu, B., Y. Fang, D.K. Xu, J. Chen, S. Ai, H. Long, and J. Cao. 2015. Investigation of material deformation mechanism in double side incremental sheet forming. *International Journal of Machine Tools and Manufacture* 93: 37–48.

Mason, B. 1978. *Sheet metal forming small batches*. Bachelor's thesis, University of Nottingham.

Matsubara, S. 2001. A computer numerically controlled dieless incremental forming of a sheet metal. *Proceedings of the Institution of Mechanical Engineers, Part B: Journal of Engineering Manufacture* 215 (7): 959–966.

Milutinovića, M., R.L.M. Potranb, D. Vilotića, P. Skakuna, and M. Plančaka. 2014. Application of single point incremental forming for manufacturing of denture base. *Journal for Technology of Plasticity* 39 (2): 15–23.

Mirnia, M.J., B.M. Dariani, H. Vanhove, and J.R. Duflou. 2014. Thickness improvement in single point incremental forming deduced by sequential limit analysis. *The International Journal of Advanced Manufacturing Technology* 70 (9–12): 2029–2041.

Nguyen-Tran, H.D., H.S. Oh, S.T. Hong, H.N. Han, J. Cao, S.H. Ahn, and D.M. Chun. 2015. A review of electrically-assisted manufacturing. *International Journal of Precision Engineering and Manufacturing-Green Technology* 2 (4): 365–376.

Nirala, H. K, Paul, A., Singh, A., Agrawal, A. 2015. Adaptive step depth for uniform stretching in single point incremental forming. In *International Conference on Precision, Meso, Micro and Nano Engineering (COPEN 2015)*, December 10–12, IIT Bombay, India.

Nirala, Harish Kumar, and Anupam Agrawal. 2016. Approach for prediction and calculation of sheet thinning in incremental sheet forming (AIMTDR-2016), December 16–18, 2016 at College of Engineering, Pune, Maharashtra, INDIA.

Nirala, H.K., P.K. Jain, J.J. Roy, M.K. Samal, and P. Tandon. 2017. An approach to eliminate stepped features in multi-stage incremental sheet forming process: Experimental and FEA analysis. *Journal of Mechanical Science and Technology* 31 (2): 599–604.

Paniti, I., & Paroczi, A. 2011. Design and modeling of integrated hall-effect sensor based on-line thickness measurement device for incremental sheet forming processes. In *2011 IEEE/ASME International Conference on Advanced Intelligent Mechatronics (AIM)*, 297–302. IEEE.

Piegl, L., and W. Tiller. 1997. *The NURBS book (Monographs in visual communication)*, 2nd ed. New York: Springer.

Silva, M.B., M. Skjodt, A.G. Atkins, N. Bay, and P.A.F. Martins. 2008a. Single-point incremental forming and formability—Failure diagrams. *The Journal of Strain Analysis for Engineering Design* 43 (1): 15–35.

Silva, M.B., M. Skjodt, P.A. Martins, and N. Bay. 2008b. Revisiting the fundamentals of single point incremental forming by means of membrane analysis. *International Journal of Machine Tools and Manufacture* 48 (1): 73–83.

Silva, M.B., P.S. Nielsen, N. Bay, and P.A. Martins. 2011. Failure mechanisms in single-point incremental forming of metals. *The International Journal of Advanced Manufacturing Technology* 56 (9–12): 893–903.

Skjodt, M., M.B. Silva, P.A.F. Martins, and N. Bay. 2010. Strategies and limits in multi-stage single-point incremental forming. *The Journal of Strain Analysis for Engineering Design* 45 (1): 33–44.

Xu, D., R. Malhotra, N.V. Reddy, J. Chen, and J. Cao. 2012. Analytical prediction of stepped feature generation in multi-pass single point incremental forming. *Journal of Manufacturing Processes* 14 (4): 487–494.

Young, D., and J. Jeswiet. 2004. Wall thickness variations in single-point incremental forming. *Proceedings of the Institution of Mechanical Engineers, Part B: Journal of Engineering Manufacture* 218 (11): 1453–1459.